Chemical Engineering Journal 145 (2009) 377–384

Contents lists available at ScienceDirect

Chemical Engineering Journal

journal homepage: www.elsevier.com/locate/cej

Modeling and experimental studies on absorption of CO_2 by Benfield solution in rotating packed bed

Fei Yi[a,b,1], Hai-Kui Zou[a,b], Guang-Wen Chu[a,b], Lei Shao[a,b], Jian-Feng Chen[a,b,*]

[a] Research Center of the Ministry of Education for High Gravity Engineering and Technology, Beijing University of Chemical Technology, Beijing 100029, PR China
[b] Key Lab for Nanomaterials, Ministry of Education, Beijing University of Chemical Technology, Beijing 100029, PR China

ARTICLE INFO

Article history:
Received 27 February 2008
Received in revised form 5 August 2008
Accepted 5 August 2008

Keywords:
Modeling
Rotating packed bed
Gas–liquid mass transfer
Absorption
Carbon dioxide
End effect

ABSTRACT

This work presents the modeling and experimental investigation on absorption of CO_2 by Benfield solution in rotating packed bed (RPB). A model was established to illustrate the mechanism of gas–liquid mass transfer with reactions in RPB at higher gravity level. Experiments were carried out at various rotating speeds, liquid flow rates, gas flow rates and temperatures in RPB, with Benfield solution as the absorbent. The validity of this model was demonstrated by the fact that most of the predicted y_o (mole fraction of CO_2 in outlet gas) agreed well with the experimental data with a deviation within 10%. The presented profile of $K_G a$ (gas-phase volumetric mass transfer coefficient) along the radial direction of the packing could reasonably explain the end effect in RPB. As a result, this model is reliable in describing the removal of CO_2 by Benfield solution in RPB at higher gravity level.

1. Introduction

CO_2 is a greenhouse gas and a main contributing factor to the global warming. In order to reduce CO_2 emission, more than 140 countries have ratified the Kyoto Protocol, which was validated on February 16, 2005. So far, researchers have developed several methods to remove CO_2, such as absorption, adsorption and membrane [1]. Absorption process has been industrially adopted in many processes, such as synthesis-gas production, natural gas processing, oil refining, and hydrogen manufacture. The conventional gas–liquid contactors employed in those processes, including packed tower, spray column, and bubble column, have significant limitations in mass transfer, leading to low efficiency and high cost. Therefore, the development of a gas–liquid contactor with high mass transfer efficiency is desired.

Rotating packed bed (RPB), also known as Higee (High gravity), is used as a gas–liquid contactor for the applications of reactive precipitation, distillation, stripping, etc [2–4]. According to previous studies, RPB has higher gas–liquid mass transfer efficiency, which is evidenced by the fact that the volumetric gas–liquid mass transfer coefficients achieved in RPB are an order of magnitude higher than those in conventional packed bed [5,6] RPB is designed to generate high acceleration via centrifugal force, leading to the formation of thin liquid films and tiny liquid droplets, which could enhance the mass transfer between gas and liquid. Recently, RPB has been used to absorb CO_2 with aqueous solutions of alkanolamine as absorbents [7,8], and the effects of various operation parameters on the absorption performances were investigated.

In the manufacture of ammonia, the removal of CO_2 from the synthesis gas is an important step. Benfield Process, originally developed by Benson et al. [9], has gained wide industrial acceptance for CO_2 removal. In Benfield Process, amine-promoted hot potassium carbonate solution, which is called Benfield solution, is employed as the absorbent. The amine promoter could significantly enhance the absorption rate, while the carbonate–bicarbonate buffer offers advantages of large capacity for CO_2 absorption and ease of regeneration. Therefore, Benfield Process is known as an economic and efficient way of removing large quantities of CO_2 from synthesis gases. Conventional packed bed has been used as the gas–liquid contactor for Benfield Process for a long time and attempts have been made to model this process. A model proposed by Sanyal et al. [10] simplified the calculations and gave reasonable predictions for Benfield Process in packed bed.

A few authors have attempted to establish the model of gas–liquid mass transfer in RPB as well. Guo et al. [11] developed a model describing three types of mass transfer processes in a cross-flow RPB. Chen et al. [12] proposed a model for ozonation process in

* Corresponding author at: Beijing University of Chemical Technology, P.O. Box 176, Beijing 100029, PR China. Tel.: +86 10 64446466; fax: +86 10 64434784.
E-mail addresses: fyi@wustl.edu (F. Yi), chenjf@mail.buct.edu.cn (J.-F. Chen).
[1] Present address: Washington University in St. Louis, MO, USA. Tel. 01-314-935-8521.

1385-8947/$ – see front matter © 2008 Published by Elsevier B.V.
doi:10.1016/j.cej.2008.08.004

Nomenclature

a_t	specific area of packing per unit volume of a packed bed ($m^2\ m^{-3}$)
c	concentration of CO_2 in a spheral droplet ($kmol\ m^{-3}$)
c_{CO_2}	concentration of CO_2 in the reactive solution ($kmol\ m^{-3}$)
$c_{CO_2,e}$	equilibrium concentration of CO_2 in the reactive solution ($kmol\ m^{-3}$)
c_{DEA}	concentration of DEA ($kmol\ m^{-3}$)
c_e	equilibrium concentration of CO_2 in a spheral droplet ($kmol\ m^{-3}$)
$c_{HCO_3^-}$	concentration of HCO_3^- ion ($kmol\ m^{-3}$)
c_{OH^-}	concentration of OH^- ion ($kmol\ m^{-3}$)
c_0	concentration of CO_2 at the gas–liquid interface ($kmol\ m^{-3}$)
d	diameter of spheral droplet (m)
d_p	packing nominal size (m)
d_1	the diameter of droplets at demarcation point (m)
D_G	diffusivity of CO_2 in gas ($m^2\ s^{-1}$)
D_L	diffusivity of CO_2 in the reactive solution ($m^2\ s^{-1}$)
g_0	characteristic centrifugal acceleration (=100 $m\ s^{-2}$) ($m\ s^{-2}$)
G'	gas mass flux ($kg\ m^{-2}\ s^{-1}$)
G_{N_2}	molar flow rate of N_2 ($mol\ s^{-1}$)
h	axial height of a packed bed (m)
h_i	ion-specific parameter ($m^3\ kmol^{-1}$)
h_G	gas-specific parameter ($m^3\ kmol^{-1}$)
H	Henry's constant in the reactive solution ($Pa\ m^3\ mol^{-1}$)
H_0	Henry's constant in pure water ($Pa\ m^3\ mol^{-1}$)
k_{DEA}	forward rate constant of Reaction (13) ($m^3\ kmol^{-1}\ s^{-1}$)
k_G	gas-side mass transfer coefficient ($mol\ Pa^{-1}\ m^{-2}\ s^{-1}$)
k_L	liquid-side mass transfer coefficient ($m\ s^{-1}$)
k_{OH}	forward rate constant of Reaction (4) ($m^3\ kmol^{-1}\ s^{-1}$)
k_{-OH}	backward rate constant of Reaction (4) ($m^3\ kmol^{-1}\ s^{-1}$)
k_1	pseudo first order rate constant (s^{-1})
K_G	overall gas–liquid mass transfer coefficient ($mol\ Pa^{-1}\ m^{-2}\ s^{-1}$)
K_Ga	gas-phase volumetric mass transfer coefficient ($mol\ Pa^{-1}\ m^{-3}\ s^{-1}$)
K_w	ionic product of water ($kmol^2\ m^{-6}$)
K_1	first ionization equilibrium constant for carbonic acid ($kmol\ m^{-3}$)
K_2	second ionization equilibrium constant for carbonic acid ($kmol\ m^{-3}$)
N_{CO_2}	absorption rate of CO_2 per unit volume ($mol\ m^{-3}\ s^{-1}$)
P	total pressure (Pa)
Q	liquid flow rate ($L\ h^{-1}$)
r	radial coordinate of a packed bed from the center (m)
r_i	inner radius of a rotating packed bed (m)
r_o	outer radius of a rotating packed bed (m)
r^*	dimensionless form of r ($(r-r_i)/(r_o-r_i)$)
R	radial coordinate of a spheral droplet (m)
T	temperature (K)
u	liquid flow rate per unit area ($m\ s^{-1}$)
u_0	characteristic flow rate per unit area (=1 $cm\ s^{-1}$) ($m\ s^{-1}$)
y	mole fraction of CO_2 in gas
y_o	mole fraction of CO_2 in outlet gas

Greek letters

ε	voidage of the dry packing
ε_L	liquid holdup in RPB
μ_G	viscosity of gas ($kg\ m^{-1}\ s^{-1}$)
ρ_G	density of gas ($kg\ m^{-3}$)
ρ_L	density of liquid ($kg\ m^{-3}$)
σ	surface tension of the liquid ($N\ m^{-1}$)
υ	kinematic viscosity of the liquid ($m^2\ s^{-1}$)
υ_0	characteristic kinematic viscosity (=10^{-6} $m^2\ s^{-1}$) ($m^2\ s^{-1}$)
ω	rotational speed ($rad\ s^{-1}$)

Dimensionless quantities

Re_G	gas Reynolds number ($G'a_t^{-1}\mu_G^{-1}$)
Sc_G	gas Schmidt number ($\mu_G\rho_G^{-1}D_G^{-1}$)

RPB to achieve some empirical correlations. Nevertheless, all these works were based on the assumption of a homogeneous regime in RPB, which means some of the hydrodynamics parameters, such as liquid hold-up, film thickness, were assumed as constants. In fact, these parameters change along the radial direction of the packing in RPB. In addition, these models only predicted the mean mass transfer coefficients, so some important characteristic phenomena in RPB were ignored, such as end effect, which was experimentally discovered in the works of Guo [13] and Chen et al. [14]. Hence, a comprehensive model reflecting more realistically mass transfer mechanism in RPB needs to be developed.

The objective of the present study is to model and investigate the removal of CO_2 by Benfield solution in RPB. At first, a mechanism model was presented to describe the gas–liquid mass transfer process with reactions in RPB operated at higher gravity level. The experiments of CO_2 absorption by Benfield solution in RPB at various operation conditions were carried out as well. The validity of the model is demonstrated by the agreement of the predicted results with the experimental data. Moreover, the model could reasonably illustrate end effect in RPB and provide much valuable information about the removal of CO_2 by Benfield solution in RPB at higher gravity level.

2. Chemical reactions

The basic reaction chemistry for hot potassium carbonate solution and CO_2 is represented by the following overall reaction:

$$CO_2 + K_2CO_3 + H_2O \rightleftarrows 2KHCO_3 \quad (1)$$

Since potassium carbonate and potassium bicarbonate are both strong electrolytes, it may be assumed that the metal is present only in the form of K^+ ions, and Reaction (1) can be more realistically represented in the ionic terms as

$$CO_2 + CO_3^{2-} + H_2O \rightleftarrows 2HCO_3^- \quad (2)$$

The above reaction, being trimolecular, evidently involves a sequence of elementary steps. At high pH (pH > 10), it is composed of the following two reactions [15]:

$$CO_3^{2-} + H_2O \rightleftarrows OH^- + HCO_3^- \quad (3)$$

$$CO_2 + OH^- \underset{k_{-OH}}{\overset{k_{OH}}{\rightleftarrows}} HCO_3^- \quad (4)$$

Since Reaction (3) is an instantaneous reaction, Reaction (4) is the rate-controlling step. Thus, the rate equation for reaction of CO_2 with un-promoted hot potassium carbonate can be written as

$$-r_{OH} = k_{OH} c_{OH^-} c_{CO_2} - k_{-OH} c_{HCO_3^-} \quad (5)$$

where k_{OH} and k_{-OH} are forward and backward rate constants of Reaction (4), respectively. When chemical equilibrium is reached, Eq. (5) gives:

$$k_{OH} c_{OH^-} c_{CO_2,e} = k_{-OH} c_{HCO_3^-} \quad (6)$$

where $c_{CO_2,e}$ is the equilibrium concentration of CO_2. The reaction rate for reverse Reaction (4) in Eq. (6) has been evaluated by considering conditions at equilibrium, and it is generally true even when the system is not at equilibrium [16]. The net forward rate of reaction can be deduced by substituting Eq. (6) into Eq. (5):

$$-r_{OH} = k_{OH} c_{OH^-} (c_{CO_2} - c_{CO_2,e}) \quad (7)$$

$c_{CO_2,e}$ can be calculated from the ionization of carbonic acid:

$$CO_2 + H_2O \overset{K_1}{\rightleftarrows} HCO_3^- + H^+ \quad (8)$$

$$HCO_3^- \overset{K_2}{\rightleftarrows} CO_3^{2-} + H^+ \quad (9)$$

Therefore, $c_{CO_2,e}$ can be written as

$$c_{CO_2,e} = \frac{K_2 c_{HCO_3^-}^2}{K_1 c_{CO_3^{2-}}} \quad (10)$$

where K_1 and K_2 is the first and second ionization constant of carbonic acid, respectively. Taking into account the ionization equilibrium of water:

$$H_2O \overset{K_w}{\rightleftarrows} H^+ + OH^- \quad (11)$$

the OH^- concentration can therefore be expressed as

$$c_{OH^-} = \frac{K_w c_{CO_3^{2-}}}{K_2 c_{HCO_3^-}} \quad (12)$$

where K_w is the equilibrium constant of the ionization equilibrium of water.

When a small amount of diethanolamine (DEA) is added into the solution, the absorption rate of CO_2 is enhanced significantly according to the following reactions [17]:

$$CO_2 + R_2NH \overset{k_{DEA}}{\rightleftarrows} R_2N^+HCOO^- \quad (13)$$

$$R_2N^+HCOO^- + OH^- \rightleftarrows R_2NH + HCO_3^- \quad (14)$$

CO_2 reacts with DEA to form carbamate, a zwitterion intermediate, in Reaction (13), which is followed by Reaction (14) to regenerate DEA by reacting carbamate with OH^-. Reaction (13) is much faster than Reaction (14) at ambient temperature. However, the reaction rate of Reaction (14) increases significantly and Reaction (13) becomes the rate-controlling step at high temperatures in industrial operation conditions [15,18]. Furthermore, the above system is better represented by a homogeneous catalysis mechanism at high temperatures. The rate equation for r_{DEA} can be obtained by using the same approach for deriving Eq. (7):

$$-r_{DEA} = k_{DEA} c_{DEA} (c_{CO_2} - c_{CO_2,e}) \quad (15)$$

where k_{DEA} are forward rate constant of Reaction (13).

Adding Eq. (7) to Eq. (15) leads to the overall pseudo-first order rate equation of CO_2 with promoted hot potassium carbonate in liquid phase:

$$-r_{CO_2} = (k_{OH} c_{OH^-} + k_{DEA} c_{DEA})(c_{CO_2} - c_{CO_2,e}) = k_1 (c_{CO_2} - c_{CO_2,e}) \quad (16)$$

where k_1 is the overall apparent first-order rate constant and defined as

$$k_1 = k_{OH} c_{OH^-} + k_{DEA} c_{DEA} \quad (17)$$

3. Model development

The forms of liquid flow in RPB were observed to fall into three main types: film flow, pore flow and droplet flow. In Burns' study, droplet flow was the main form of liquid flow in RPB when the rotating speed was approximately above 800 rpm (the centrifugal acceleration is 684 m s^{-2} based on the arithmetic mean radii of the RPB) [19]. The higher the rotating speed is, the larger the proportion of liquid flowing in the form of droplets is. In the present study, if the centrifugal acceleration based on the arithmetic mean radii of the RPB is above 600 m s^{-2} (60 g), which is the case in most industrial applications, it could be regarded that the RPB reaches higher gravity level. In this model, it is assumed that the liquid moving in the RPB at higher gravity level only exists in the form of spheral droplets.

After assuming that all the liquid flows as spheral droplets, mass transfer in a single droplet should be analyzed clearly. Carbonate–bicarbonate system is a buffer solution, so the concentration of OH^- does not change much in these small spheral droplets, and k_1 can be assumed as a constant in a spheral droplet. Since the conversion of potassium carbonate into potassium bicarbonate is very low in a small droplet, $c_{CO_3^{2-}}$ and $c_{HCO_3^-}$ are also assumed as constants in the droplet. Therefore, the equilibrium concentration of CO_2 could be treated as a constant in a droplet according to Eq. (10). The mass balance of CO_2 in a spheral droplet can be thus expressed as

$$\frac{\partial c}{\partial t} = \frac{D_L}{R^2} \frac{\partial}{\partial R} \left(R^2 \frac{\partial c}{\partial R} \right) - k_1 (c - c_e) \quad (18)$$

Considering CO_2 reacts very fast with OH^- and DEA, based on the high value of k_1 at temperatures in this study, it takes very short time for the concentration of CO_2 in liquid phase to reach steady-state. Thus, omitting $\partial c/\partial t$ can convert Eq. (18) into an ordinary differential equation:

$$\frac{D_L}{R^2} \frac{d}{dR} \left(R^2 \frac{dc}{dR} \right) - k_1 (c - c_e) = 0 \quad (19)$$

The boundary conditions are

$$c\left(\frac{d}{2}\right) = c_0; \qquad \left.\frac{dc}{dR}\right|_{R=0} = 0 \quad (20)$$

where c_0 is the dissolved CO_2 concentration at the gas–liquid interface.

The solution to Eq. (19) is

$$c = (c_0 - c_e) \frac{d}{2R} \frac{\sinh(\sqrt{(k_1/D_L)}R)}{\sinh(\sqrt{(k_1/D_L)}(d/2))} + c_e \quad (21)$$

Fig. 1 shows the concentration profile of CO_2 calculated by Eq. (21) in a spheral droplet with a diameter of 5.4×10^{-5} m at 356 K. The concentration of CO_2 quickly reduces to c_e from the gas–liquid interface to the inner part of the droplet. Obviously, most of CO_2 is consumed in the liquid film close to the interface. Furthermore,

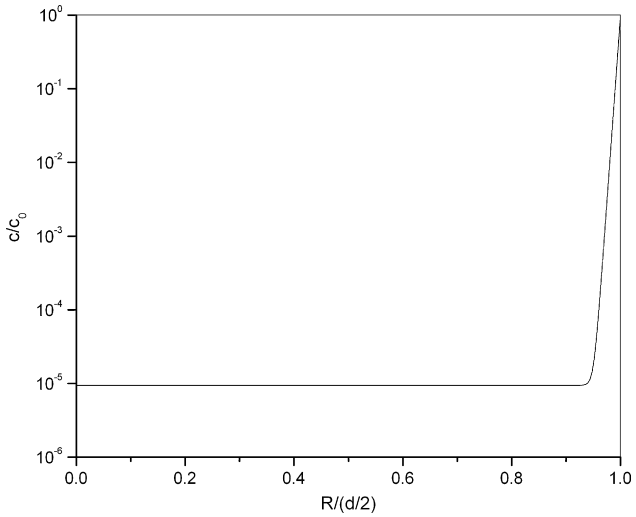

Fig. 1. Concentration profile of CO_2 in a spheral droplet.

liquid-side mass transfer coefficient (k_L) can be calculated from the following equation:

$$k_L(c_0 - c_e) = D_L \left.\frac{dc}{dR}\right|_{R=d/2} \tag{22}$$

Therefore, k_L is written as

$$k_L = D_L \left(\frac{\sqrt{k_1/D_L}}{\tanh((\sqrt{k_1/D_L}(d/2)) - (2/D))} \right) \tag{23}$$

Previous study reported that the gas flow in RPB is akin to that in conventional packed beds [20] and the values of gas-side mass transfer coefficient (k_G) in RPB lie in a range similar to those in conventional packed beds [21]. Hence, k_G in RPB can be estimated by the equation proposed by Onda et al. [22]:

$$\frac{k_G RT}{a_t D_G} = 2Re_G^{0.7} Sc_g^{1/3} (a_t d_p)^{-2.0} \tag{24}$$

The overall gas–liquid mass transfer coefficient (K_G) of RPB can be determined by the following equation:

$$\frac{1}{K_G} = \frac{1}{k_G} + \frac{H}{k_L} \tag{25}$$

The liquid holdup in RPB is evaluated by the correlation proposed by Burns et al. [23]:

$$\varepsilon_L = 0.039 \left(\frac{\omega^2 r}{g_0}\right)^{-0.5} \left(\frac{u}{u_0}\right)^{0.6} \left(\frac{\nu}{\nu_0}\right)^{0.22} \tag{26}$$

where $g_0 = 100\,m\,s^{-2}$, $u_0 = 1\,cm\,s^{-1}$, and $\upsilon_0 = 10^{-6}\,m^2\,s^{-1}$.

In the previous work from our group, Zhang [24] took a large number of pictures of flowing liquid in RPB by a stroboscope and quantitatively analyzed the size of droplets. The whole packing zone was divided into two parts: end effect zone (the part of the packing close to the inner edge of the rotator) and bulk packing zone (the rest zone of the packing). The variation patterns of the droplet diameter in the two zones were different. The demarcation point between end effect zone and bulk packing zone was experimentally observed at about 10 mm from the inner edge of the rotator. In the inner part of end effect zone, the diameter of droplets was very small due to the intense impingement between liquid and the packing. Because of the smaller flow area in end effect zone, droplets had more possibility to coalesce than those in bulk packing zone. The diameter of droplets in end effect zone grew moderately when liquid flowed outward in the packing, and the diameter of droplets at the inner edge of end effect zone was experimentally found to be 0.826 d_1 [24]. In this model, it is assumed that the diameter of droplets grows linearly in end effect zone. Thus, the expression gives:

$$d = (0.826 + 17.4(r - r_i))d_1, \quad r - r_i < 0.01m \tag{27}$$

In bulk packing zone, the flow area increases as liquid flows outward, so the possibility of coalescence between droplets is relatively small. Due to the incision of the packing against liquid, the diameter of droplets decreases with the increase of r. In addition, Guo et al. concluded that liquid flow was independent of gas flow in RPB from experimental investigation [25]. Therefore, based on Zhang's data, which is referable since the high gravity level in this study lay in the same range as that in Zhang's and the packing was also identical, the diameter of droplets in bulk packing zone is regressed as follows:

$$d = 12.84 \left(\frac{\sigma}{\omega^2 r \rho}\right)^{0.630} u^{0.201}, \quad r - r_i \geq 0.01m \tag{28}$$

Fig. 2 shows the diameter profile of droplets in RPB calculated by Eqs. (27) and (28) with the inner radius of the packing as 40 mm and the outer radius of the packing as 100 mm, which are the parameters of the RPB employed in this study, and the operation conditions of liquid flow rate of 79.70 L h^{-1}, rotating speed of 900 rpm and temperature of 356 K.

The absorption rate of CO_2 per unit volume is written as

$$N_{CO_2} = K_G a(Py - c_e H) = K_G \frac{6\varepsilon_L}{d}(Py - c_e H) \tag{29}$$

Before deriving the mass balance equations, assumptions of the model for the RPB in the present study are listed as follows:

1. Steady-state condition prevails.
2. The amount of water in gas-phase is neglected.
3. The plug-flow condition is applicable to both gas and liquid phases.
4. The pressure drop in the RPB is neglected.
5. Isothermal absorption takes place in the RPB.

In this model, the concentration of every component varies only in the radial direction of the packing, because liquid and gas have little circumferential motion [18]. Liquid motion in RPB hardly has back mixing [25], so the liquid radial flow is close to plug flow. Since

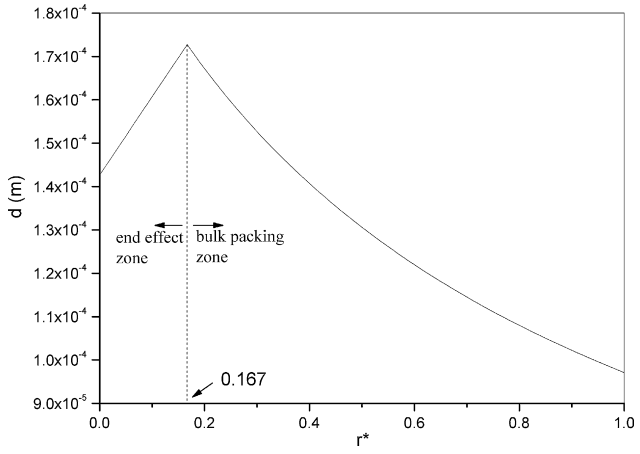

Fig. 2. The diameter profile of droplets in RPB.

Table 1
Equilibrium, kinetics and transport parameters.

Parameter	Expression	Source
H_0	$H_0 = 2.82 \times 10^6 \exp\left(-\frac{2044}{T}\right)$	[27]
H	$\lg\left(\frac{H}{H_0}\right) = \sum(h_i + h_G)c_i$	[28]
k_{OH}	$\lg k_{OH} = 13.635 - \frac{2895}{T} + 0.08I$	[29]
k_{DEA}	$\ln k_{DEA} = 27.06 - \frac{5284.4}{T}$	[18]
D_L	$\lg D_L = -7.0188 - \frac{586.9729}{T}$	[30]
D_G	$D_G = \frac{1.8583\times10^{-7}T^{3/2}}{P\sigma^2_{CO_2,N_2}\Omega_D}\left(\frac{1}{M_{CO_2}} + \frac{1}{M_{N_2}}\right)^{1/2}$	[31]
K_w	$K_w = \exp\left(39.555 - \frac{9.879\times10^4}{T} + \frac{5.6883\times10^7}{T^2} - \frac{1.4645\times10^{10}}{T^3} + \frac{1.3615\times10^{12}}{T^4}\right)$	[32]
K_1	$\lg K_1 = -\frac{3404.7}{T} + 14.843 - 0.03279T$	[33]
K_2	$K_2 = \exp\left(-294.74 + \frac{3.6439\times10^5}{T} - \frac{1.8416\times10^8}{T^2} + \frac{4.1579\times10^{10}}{T^3} - \frac{3.5429\times10^{12}}{T^4}\right)$	[32]

gas flows inward from the outer edge of the RPB by a pressure-driving force, it also has little back mixing, which makes gas radial flow close to plug flow as well. In this one-dimensional mass transfer model, the pressure drop in RPB can be neglected because it is very small compared to the whole pressure [26]. Though the absorption reaction of CO_2 is exothermic, we can still neglect the variation on temperatures of both gas and liquid due to the low conversion, which was experimentally verified by the small variation in temperatures between inlet and outlet streams of gas and liquid. In addition, mass transfer in the casing was neglected due to the low mass transfer coefficient in that zone [13].

On the basis of the above assumptions, a differential mole balance in gas-phase for CO_2 gives the following equation:

$$G_{N_2} d\left(\frac{y}{1-y}\right) = N_{CO_2} 2\pi r h dr \tag{30}$$

In liquid phase, K_2CO_3 is consumed by chemical reaction and $KHCO_3$ is the reaction product as the solution moves outward in RPB. Hence, when the reaction stoichiometry is taken into account, differential mole balance for K_2CO_3 and $KHCO_3$ gives:

$$d(Qc_{CO_3^{2-}}) = -N_{CO_2} 2\pi r h dr \tag{31}$$

$$d(Qc_{HCO_3^-}) = 2N_{CO_2} 2\pi r h dr \tag{32}$$

In order to simplify the calculation, the experimental conditions with low conversion of K_2CO_3 were adopted to verify the model. Under low conversion of K_2CO_3, the increase in liquid mass is so small that the liquid flow rate (Q) hardly increases as the liquid moves outward and Q can be assumed as a constant. Eqs. (31) and (32) can be thus simplified as follows:

$$Q dc_{CO_3^{2-}} = -N_{CO_2} 2\pi r h dr \tag{33}$$

$$Q dc_{HCO_3^-} = 2N_{CO_2} 2\pi r h dr \tag{34}$$

All the equilibrium, kinetics and transport parameters are tabulated in Table 1.

4. Numerical solution

The proposed three differential Eqs. (30), (33) and (34) need to be solved to simulate CO_2 removal in RPB by taking into account the boundary conditions. The flow rate, composition and temperature of the gas entering the RPB at its outer edge and the flow rate, concentration and temperature of the liquid entering the RPB at its

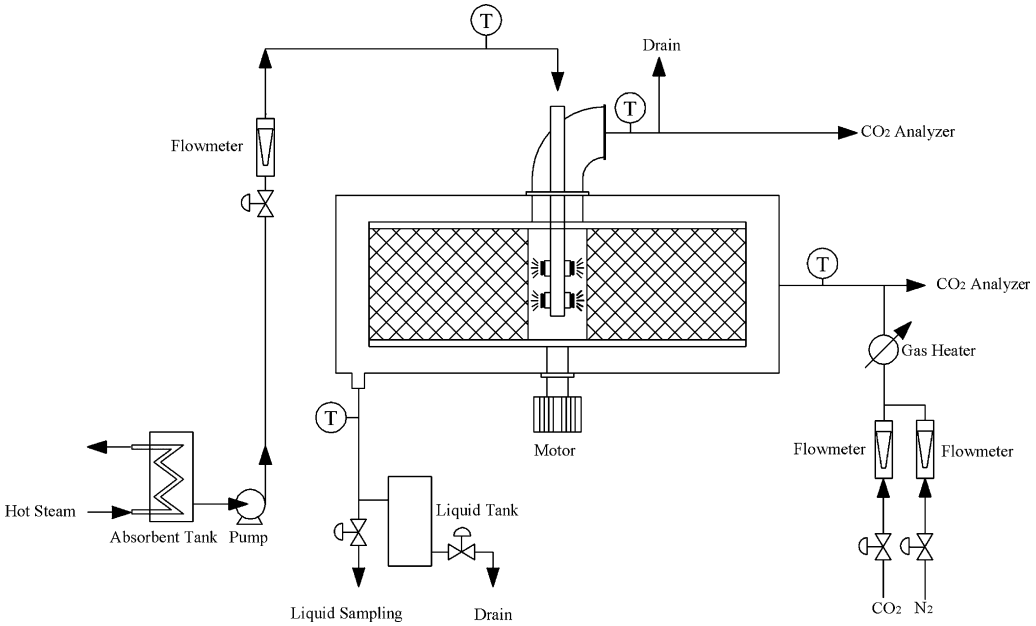

Fig. 3. Experimental setup for CO_2 absorption in RPB.

Table 2
Specification of the RPB used in this study.

Item	RPB
Inner radius of the packing, r_i (m)	0.040
Outer radius of the packing, r_o (m)	0.100
Axial length of the packing, h (m)	0.031
Volume of the packing, V_B (m^3)	8.18×10^{-4}
Surface area of per unit volume of the dry packing, a_t ($m^2\ m^{-3}$)	870
Voidage of the dry packing, ε ($m^3\ m^{-3}$)	0.95

inner edge are known in simulation problem. To start the integration procedure, the composition of the gas exiting the RPB from its inner edge needs to be estimated. With the help of the estimated values, the equations can be integrated by Runge-Kutta method up to the outer edge of the RPB. Using shooting method, a new value of CO_2 composition in the outlet gas was estimated for the further iteration until satisfactory convergence was obtained. A MATLAB program was used to solve the model equations.

5. Experimental

Fig. 3 depicts the experimental apparatus for CO_2 absorption, and the specification of the RPB is given in Table 2. Stainless wire mesh was used as the packing. Before the gas and liquid entered the RPB, they were preheated to the same temperature. The nitrogen gas stream containing CO_2 flowed inward from the outer edge of the RPB by a pressure-driving force and the aqueous absorbent was sprayed through 10 holes in the liquid distributor at the center of RPB. These 10 holes, directly facing the packing, are arranged in a vertical group of 5 and the groups are spaced 180° apart. The aqueous absorbent moved outward and left from the outer edge of the RPB through a centrifugal force. Gas and liquid streams contacted counter currently in the RPB and CO_2 in the gas stream was dissolved and reacted with the absorbent in the liquid stream before the gas and liquid streams left the RPB from gas outlet and liquid outlet, respectively.

In the present study, the pressure of inlet gas was maintained at 0.40 MPa. Temperature of the inlet liquid and gas streams ranged from 356 to 375 K. The mass fraction of K_2CO_3 and DEA in the inlet aqueous absorbent was 27% and 4%, respectively. In order to maintain higher gravity level, the rotating speed varied from 900 to 1300 rpm, providing a centrifugal acceleration from 622 to 1298 $m\ s^{-2}$ based on the arithmetic mean radii of RPB. For all the runs, a steady-state operation was reached within 5 min. Fig. 4 shows dynamic variation of CO_2 concentration in outlet gas in an experiment under the operation conditions of rotating speed of 1300 rpm, liquid flow rate of 79.70 L h^{-1}, gas flow rate of 0.481 mol min^{-1}, inlet CO_2 concentration of 4.10 mol% and temperature of 356 K. The CO_2 concentrations in the inlet and outlet gas streams were measured by two infrared gas analyzers (GXH-3010F, Huayun Analytical Instrument Institution, CO_2 mole fraction ranged from 0% to 10%). The concentrations of K_2CO_3 and $KHCO_3$ in the outlet liquid stream were determined by pH potentiometric titration method. Sulfuric acid standard solution was used as the acid solution.

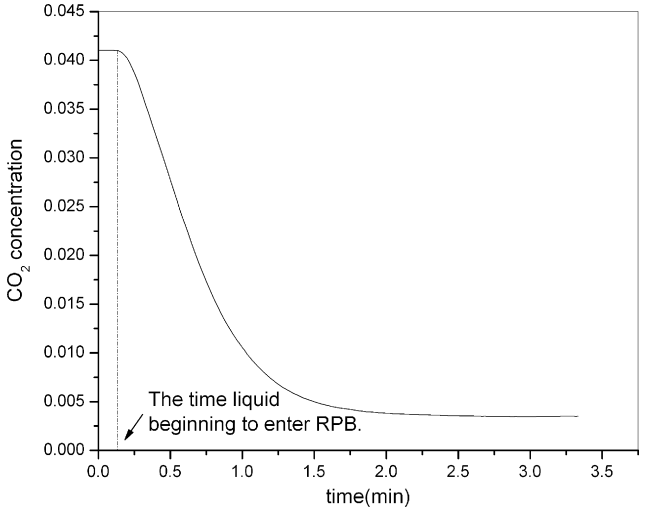

Fig. 4. CO_2 concentration in outlet gas versus time.

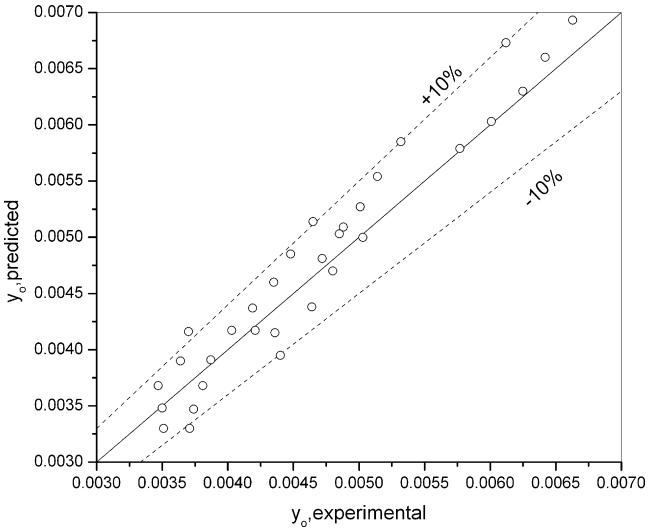

Fig. 5. Diagonal graph of experimental and predicted y_o.

DEA was purchased from Tianjin Kernel Chemical Reagents Development Center, and potassium carbonate was purchased from Tianjin Ruijinte Chemicals Co. Ltd. These chemicals have a purity of 99.9% and were used in the experiments without further purification. Both CO_2 and N_2 with a purity of 99.9% were bought from Daqing Xuelong Co.

6. Model validation

Fig. 5 is the diagonal plot of the predicted and experimental values of CO_2 composition in the outlet gas. It can be found that this model offers relatively precise predictions on CO_2 removal in RPB, with a deviation within 10% compared to the experimental values.

7. Results and discussion

7.1. Effect of liquid flow rate

Fig. 6 shows the dependence of gas-phase volumetric mass transfer coefficient ($K_G a$) on the liquid flow rate under the operation conditions of rotating speed of 1300 rpm, gas flow rate of 0.481 mol min^{-1}, inlet CO_2 concentration of 4.10 mol% and temperature of 356 K. It is seen that $K_G a$ increased with an increase in liquid flow rate from 44.28 to 79.70 L h^{-1}. An increase in liquid flow rate increased k_L, which means that the liquid-side mass transfer resistance reduced. Besides, a larger liquid flow rate caused an increase in liquid holdup, providing more gas–liquid contact area. Both of the factors led to the increase of $K_G a$.

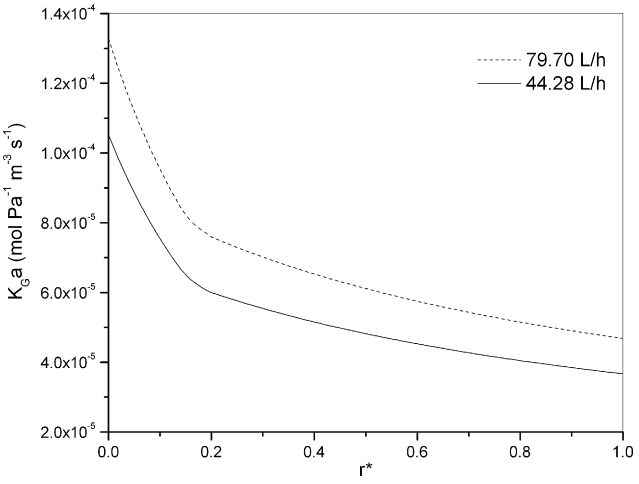

Fig. 6. Effect of the liquid flow rate on $K_G a$ in RPB.

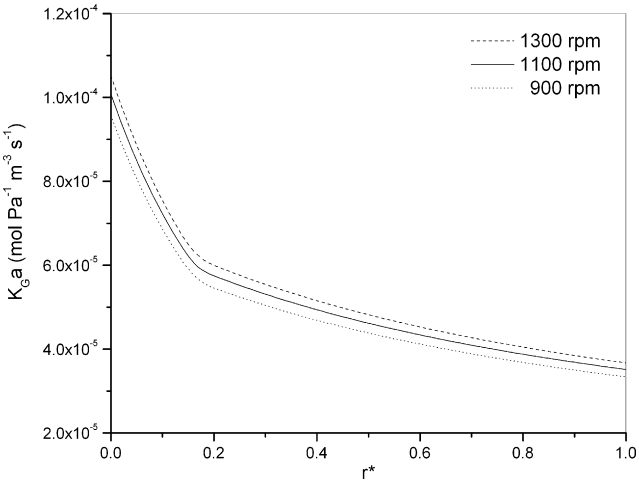

Fig. 8. Effect of the rotating speed on $K_G a$ in RPB.

7.2. Effect of gas flow rate

Fig. 7 shows the dependence of $K_G a$ on the gas flow rate under the operation conditions of rotating speed of 1000 rpm, liquid flow rate of 61.99 L h^{-1}, inlet CO_2 concentration of 2.90 mol% and temperature of 356 K. It is seen that $K_G a$ increased with an increase in gas flow rate from 0.690 to 0.920 mol min^{-1}. Increasing gas flow rate could reduce the gas-side mass transfer resistance, resulting in an increase in $K_G a$.

7.3. Effect of rotating speed

Fig. 8 shows the dependence of $K_G a$ on the rotating speed under the operation conditions of liquid flow rate of 44.28 L h^{-1}, gas flow rate of 0.481 mol min^{-1}, inlet CO_2 concentration of 4.10 mol% and temperature of 356 K. It is seen that $K_G a$ increased with an increase in rotating speed in the range from 900 to 1300 rpm. With an increase in rotating speed, the diameter of spheral droplets at various r^* decreased, which led to a slight reduction in k_L. However, the gas–liquid contact area increased due to the smaller d, so it could compensate the loss in k_L and cause a larger $K_G a$ at higher rotating speed.

7.4. Effect of the temperature

Fig. 9 shows the dependence of $K_G a$ on temperature under the operation conditions of rotating speed of 1300 rpm, liquid flow rate of 70.84 L h^{-1}, gas flow rate of 0.481 mol min^{-1} and inlet CO_2 concentration of 4.50 mol%. It is seen that $K_G a$ increased with an increase in temperature from 356 to 375 K. According to the Arrhenius expression of reaction rate constant, a higher temperature increased k_{OH} and k_{DEA}, resulting in a higher k_1. On the other hand, a higher temperature reduced the solubility of CO_2 in absorbent solution, which was illustrated by an increasing H. However, the increase in k_L due to a higher k_1 overshadowed the increase in H, leading to a larger $K_G a$ at higher temperature.

7.5. End effect

Guo [13] discovered that there was an apparent end effect in a physical absorption process in RPB. In his experiment, the inner radius of the packing was kept unchanged, and the outer radius of the packing was varied, and the mean mass transfer coefficient calculated from the experimental data of thinner packing thickness was much higher. The same phenomena were also observed in Chen's study [14]. It is seen from Figs. 6–9 that the local values of $K_G a$ in end effect zone were much higher than those in bulk pack-

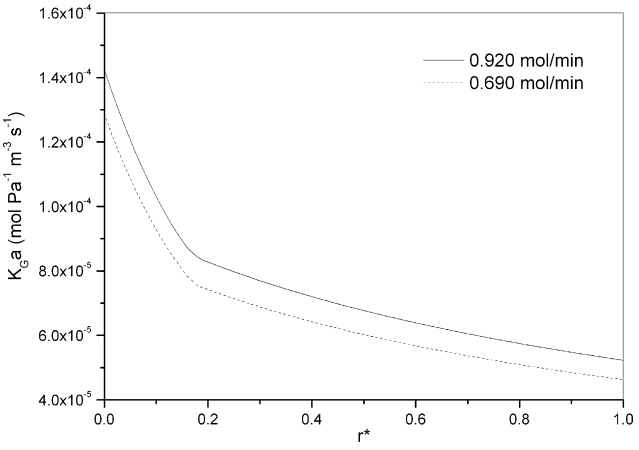

Fig. 7. Effect of the gas flow rate on $K_G a$ in RPB.

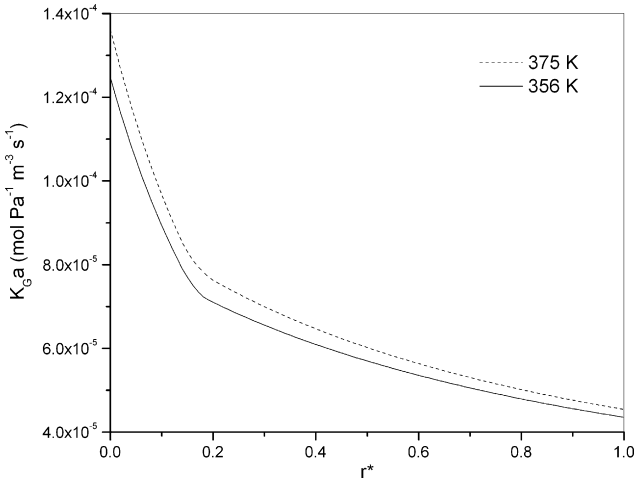

Fig. 9. Effect of the temperature on $K_G a$ in RPB.

ing zone, which demonstrates that end effect is obvious in RPB. In end effect zone, the circumferential velocity of the inlet liquid was zero before the liquid hit the packing, while the circumferential velocity of the inner edge of the packing was between 3.8 and 5.4 m s^{-1} when the rotating speed ranged from 900 to 1300 rpm in this study. Such a large relative circumferential velocity between the liquid and the packing causes intense impingement between them. Since the impingement leads to the formation of very small droplets and the liquid hold-up is relatively high in end effect zone, enormous interfacial areas are generated. Additionally, values of k_L and k_G are also relatively high in this zone. All these factors result in high values of $K_G a$ in end effect zone, which means that strong mass transfer happens in this zone.

8. Conclusion

A model was developed to simulate gas–liquid mass transfer process with reactions in RPB operated at higher gravity level in this work. This model quantitatively described the process of CO_2 removal by DEA-promoted hot potassium carbonate in RPB. The predicted values of y_o agreed well with the results from experiments at various liquid flow rates, gas flow rate, rotating speeds and temperatures. In addition, the profile of $K_G a$ along the radial direction of the packing was calculated and values of $K_G a$ decreased sharply from end effect zone to bulk packing zone. The model profiles theoretically revealed end effect in RPB, which means that RPB has much better mass transfer efficiency in the inlet region of the packing. Additionally, the effects of various operation parameters on the mass transfer efficiency in RPB at higher gravity level were predicted reasonably by this model. Furthermore, this model can be potentially used to simulate the removal of CO_2 in RPB using other aqueous absorbents.

Acknowledgements

This work was supported by the National Natural Science Foundation of China (No. 20676006), National Outstanding Youth Foundation (No. 20325621) and the National High Technology Research and Development Program of China (No. 2006AA030202 and No. 2006AA030203).

References

[1] H. Yang, Z. Xu, M. Fan, R. Gupta, R.B. Slimane, A.E. Bland, I. Wright, Progress in carbon dioxide separation and capture: a review, J. Environ. Sci. 20 (2008) 14–27.
[2] J.F. Chen, Y.H. Wang, F. Guo, X.M. Wang, C. Zheng, Synthesis of nanoparticles with novel technology: high-gravity reactive precipitation, Ind. Eng. Chem. Res. 39 (2000) 948–954.
[3] T. Kelleher, J.R. Fair, Distillation studies in a high-gravity contactor, Ind. Eng. Chem. Res. 35 (1996) 4646–4655.
[4] H.S. Liu, C.C. Lin, S.C. Wu, H.W. Hsu, Characteristics of a rotating packed bed, Ind. Eng. Chem. Res. 35 (1996) 3590–3596.
[5] S. Munjal, M.P. Dudukovic, P. Ramachandran, Mass transfer in rotating packed beds. I. Development of gas–liquid and liquid–solid mass transfer correlations, Chem. Eng. Sci. 44 (1989) 2245–2256.
[6] S. Munjal, M.P. Dudukovic, P. Ramachandran, Mass transfer in rotating packed beds. II. Experimental results and comparison with theory and gravity flow, Chem. Eng. Sci. 44 (1989) 2257–2268.
[7] C.C. Lin, W.T. Liu, C.S. Tan, Removal of carbon dioxide by absorption in a rotating packed bed, Ind. Eng. Chem. Res. 42 (2003) 2381–2386.
[8] C.S. Tan, J.E. Chen, Absorption of carbon dioxide with piperazine and its mixtures in a rotating packed bed, Sep. Purif. Technol. 49 (2006) 174–180.
[9] H.E. Benson, J.H. Field, R.M. Jimson, CO_2 absorption employing hot potassium carbonate solution, Chem. Eng. Prog. 50 (1954) 356–364.
[10] D. Sanyal, N. Vasishtha, D.N. Saraf, Modeling of carbon dioxide absorber using hot carbonate process, Ind. Eng. Chem. Res. 27 (1988) 2149–2156.
[11] F. Guo, C. Zheng, K. Guo, Y.D. Feng, N.C. Gardner, Hydrodynamics and mass transfer in cross-flow rotating packed bed, Chem. Eng. Sci. 52 (1997) 3853–3859.
[12] Y.H. Chen, C.Y. Chang, W.L. Su, C.C. Chen, C.Y. Chiu, Y.H. Yu, P.C. Chiang, S.I.M. Chiang, Modeling ozone contacting process in a rotating packed bed, Ind. Eng. Chem. Res. 43 (2004) 228–236.
[13] K. Guo, A Study on Liquid Flowing Inside the Higee Rotor, Ph.D. Dissertation, Beijing University of Chemical Technology, Beijing, China, 1996.
[14] Y.S. Chen, C.C. Lin, H.S. Liu, Mass transfer in a rotating packed bed with various radii of the bed, Ind. Eng. Chem. Res. 44 (2005) 7868–7875.
[15] G. Astarita, D.W. Savage, Promotion of CO_2 mass transfer in carbonate solutions, Chem. Eng. Sci. 36 (1981) 581–588.
[16] P.V. Danckwerts, Gas–Liquid Reactions, McGraw-Hill, New York, 1970.
[17] P.C. Tseng, D.W. Savage, Carbon dioxide absorption into promoted carbonate solutions, AIChE J. 34 (1988) 922–931.
[18] F. Leder, The absorption of CO_2 into chemically reactive solutions at high temperatures, Chem. Eng. Sci. 26 (1971) 1381–1390.
[19] J.R. Burns, C. Ramshaw, Process intensification: visual study of liquid maldistribution in rotating packed beds, Chem. Eng. Sci. 51 (1996) 1347–1352.
[20] P. Sandilya, D.P. Rao, A. Sharma, G. Biswas, Gas-phase mass transfer in a centrifugal contactor, Ind. Eng. Chem. Res. 40 (2001) 384–392.
[21] Y.S. Chen, H.S. Liu, Absorption of VOCs in a rotating packed bed, Ind. Eng. Chem. Res. 41 (2002) 1583–1588.
[22] K. Onda, H. Takeuchi, Y. Okumoto, Mass transfer coefficient between gas and liquid phases in packed columns, J. Chem. Eng. Jpn. 1 (1968) 56–62.
[23] J.R. Burns, J.N. Jamil, C. Ramshaw, Process intensification operating characteristics of rotating packed beds—determination of liquid hold-up for a high-voidage structured packing, Chem. Eng. Sci. 55 (2000) 2401–2415.
[24] J. Zhang, An Experimental and Simulation Study on Liquid Flowing and Mass Transfer in RPB, Ph.D. Dissertation, Beijing University of Chemical Technology, Beijing, China, 1996.
[25] K. Guo, F. Guo, Y.D. Feng, J.F. Chen, C. Zheng, N.C. Gardner, Synchronous visual and RTD study on liquid flow in rotating packed-bed contactor, Chem. Eng. Sci. 55 (2000) 1699–1706.
[26] M.P. Kumar, D.P. Rao, Studies on a high-gravity gas–liquid contactor, Ind. Eng. Chem. Res. 29 (1990) 917–920.
[27] G.F. Versteeg, W.P.M. van Swaaij, Solubility and diffusivity of acid gases (CO_2, N_2O) in aqueous alkanolamine solutions, J. Chem. Eng. Data 33 (1988) 29–34.
[28] S. Weisenberger, A. Schumpe, Estimation of gas solubilities in salt solutions at temperatures from 273 K to 363 K, AIChE J. 42 (1996) 298–300.
[29] G. Astarita, D.W. Savage, A. Bisio, Gas Treating with Chemical Solvents, Wiley, New York, 1983.
[30] D.W. Savage, G. Astarita, S. Joshi, Chemical absorption and desorption of carbon dioxide from hot carbonate solutions, Chem. Eng. Sci. 35 (1980) 1513–1522.
[31] J.O. Hirschfelder, R.B. Bird, B.L. Spotz, The transport properties of gases and gaseous mixtures. II, Chem. Rev. 44 (1949) 205–231.
[32] R.L. Kent, B. Elsenberg, Better data for amine treating, Hydrocarb. Process. 55 (1976) 87–90.
[33] P.V. Danckwerts, M.M. Sharma, The absorption of carbon dioxide into solutions of alkalis and amines. Hydrogen sulfide and carbonyl sulfide, Chem. Eng. (Lond.) 44 (1966) 244–280.